

# Enhanced Bioremediation of Zinc and Cadmium from Oil-Contaminated Sites Using Biochar-Amended Fungal Systems Involving *Aspergillus niveus* and *Alternaria chlamydosporigena*

Najwa Majrashi and Fuad Ameen\*

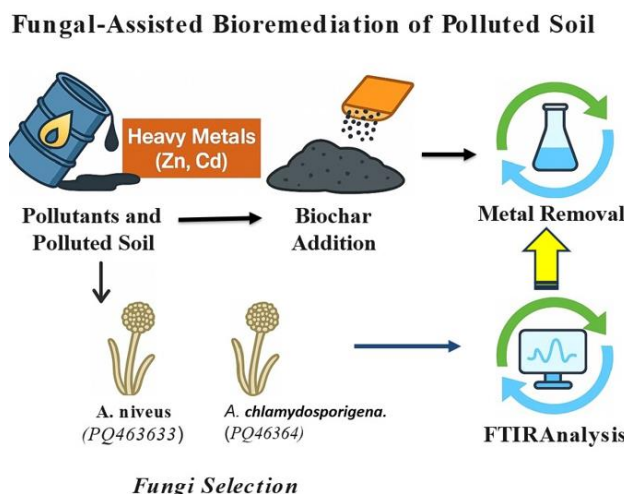
Department of Botany & Microbiology, College of Science, King Saud University, P.O. Box 2455, Riyadh 11451, Saudi Arabia

Received: 22/07/2025, Accepted: 02/02/2026, Available online: 04/02/2026

\*to whom all correspondence should be addressed: e-mail: fuadameen@ksu.edu.sa

<https://doi.org/10.30955/gnj.07853>

## Graphical abstract



## Abstract

Bioremediation of oil-contaminated sites, common in oil-producing regions, requires novel solutions, such as the one suggested here: combining fungal and biochar treatments. Fungal strains were isolated from metal and oil-polluted soils and evaluated for their resistance to zinc (Zn) and cadmium (Cd). Two strains, *Aspergillus niveus* (GenBank accession: PQ463633) and *Alternaria chlamydosporigena* (PQ463634), exhibited exceptional growth under metal stress, demonstrating considerable metal resistance. These strains were chosen for further bioremediation experiments. A substantial decrease of Zn and Cd concentrations was observed after fungal incubation. The incorporation of biochar significantly improved the effectiveness of the heavy metal removal, indicating a synergistic interaction between fungal biosorption and biochar-facilitated immobilization. Fourier-transform infrared (FTIR) spectroscopy demonstrated notable morphological and biochemical changes in the fungal biomass following exposure to Zn and Cd, signifying active metal-binding interactions and uptake processes. The equilibrium behavior of metal

uptake was demonstrated with three isotherm models. The Langmuir model showed the greatest fit ( $R^2 > 0.98$ ), followed by the Freundlich model ( $R^2 = 0.92-0.95$ ) and the Temkin model ( $R^2 = 0.85-0.89$ ). A homogenous, monolayer-driven biosorption of the metals is supported by the best fit of the Langmuir isotherm. Kinetic models were utilized to examine the rate and mechanism of the biosorption process. A high correlation coefficient ( $R^2 = 0.98$ ) for the pseudo-second-order model suggests that chemisorption is the primary mechanism for the uptake of Zn and Cd by biochar and fungi. It is concluded that the combination of biochar and the fungi *A. niveus* and *A. chlamydosporigena* offers an economical and environmentally sustainable remediation technique for soils contaminated with oil and heavy metals. The discovery is significantly advancing the creation of sustainable biotechnological approaches for environmental restoration in oil-contaminated material, providing a feasible alternative to traditional physicochemical procedures.

**Keywords:** Biochar; Bioremediation; Fungi; Heavy metal; Soil petroleum.

## 1. Introduction

Soil polluted by petroleum hydrocarbons and heavy metals is a global environmental issue. Over five million polluted sites covering ca. 500 million hectares were reported globally (Falah *et al.* 2024; Hou *et al.* 2025). The financial impact of this contamination surpasses US\$10 billion each year, with considerable consequences for ecosystems and human health. Petroleum-derived pollutants are of particular concern because they can migrate into aquatic systems and groundwater, jeopardizing the unsaturated zone and drinking water supplies. Petrogenic heavy metals, such as Pb, Zn, Ni, Mn, Cr, Fe, and Cd, exhibit enduring environmental deposition, particularly in oil-producing areas (Nna, Orie en Kalu 2024).

The region around the Arabian Gulf serves as a case study, where sixty years of oil extraction and conflict-induced

Najwa Majrashi and Fuad Ameen (2026), Enhanced Bioremediation of Zinc and Cadmium from Oil-Contaminated Sites Using Biochar-Amended Fungal Systems Involving *Aspergillus niveus* and *Alternaria chlamydosporigena*, *Global NEST Journal*, **28**(2), 07853.

**Copyright:** © 2026 Global NEST. This article is an open access article distributed under the terms and conditions of the Creative Commons Attribution International ([CC BY 4.0](https://creativecommons.org/licenses/by/4.0/)) license.

spills have resulted in severe metal contamination of coastal sediments and terrestrial ecosystems. Due to the contamination, large areas of land are unsuitable for agriculture, necessitating immediate remediation actions. Traditional methods for cleaning up the contamination, such as soil vapor extraction and thermal remediation, are too expensive and harmful to the environment, while bioremediation offers a more sustainable and cost-effective solution (Liu *et al.* 2024).

Bioremediation utilizing fungi has proven to be promising. Certain fungi such as *Aspergillus*, *Penicillium*, and *Fusarium* remove efficiently metals from the environment because of their ability to bind metals to their cell walls and store metals inside their cells (Dinakarkumar *et al.* 2024). When combined with biochar, a type of carbon produced by heating organic material, fungi can be even more efficient (W. Wang *et al.* 2024; Xia *et al.* 2025). In bioremediation *in situ*, it is important to use local microbial isolates. In the Arabian Peninsula, information on such indigenous isolates is scarce. A recent review lists bacteria and fungi isolated from petroleum refinery effluents in India, Nigeria, Malaysia, South Africa, and Iraq. In Iraq, the fungal species were *Penicillium* sp., *Aspergillus fumigatus*, *Aspergillus niger*, and *Aspergillus flavus* (Almutairi 2024). In Saudi Arabia, we found only a mention about the fungus *Scedosporium apiospermum* and the species of *Fusarium*, *Verticillium*, *Purpureocillium*, and *Clavispora* that were shown to have potential bioremediation ability of heavy metal and oil-polluted material (Ameen *et al.* 2024). In the area where oil pollution is the main source of heavy metals, novel heavy metal-resistant isolates growing under oil pollution are needed. This information is still lacking. In this study, novel indigenous fungal isolates were searched from oil-polluted soil.

To understand how well biochar and fungi can remove Zn and Cd from polluted material, we need to look at the biosorption equilibrium. Isotherm models are used to represent the distribution of metal ions between the liquid and solid phases when the system is in equilibrium (Mir en Rather 2024; Sarangi en Rajkumar 2024). The Langmuir, Freundlich, and Temkin isotherm models are used to investigate the equilibrium biosorption behavior of the metals (Dhaka *et al.* 2024).

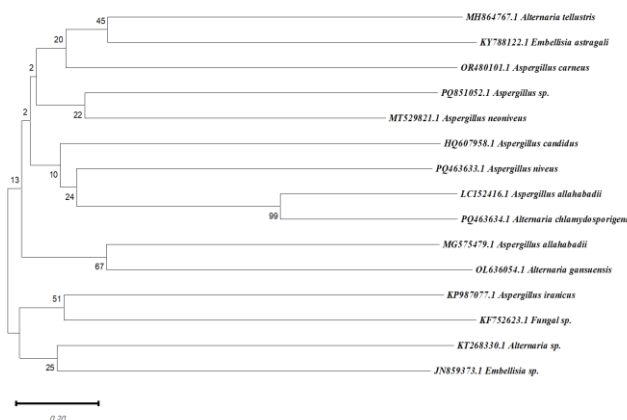


**Figure 1.** Phylogenetic tree of the fungal taxa obtained using the Neighbor-Joining method using the MEGA11 software.

Our research aimed to present a sustainable bioremediation technique for heavy metal contamination in oil-polluted material. To achieve this, the following objectives were stated. First, potential heavy metal-resistant isolates were screened from contaminated soils, and the best-performing were selected for a bioremediation experiment. Second, two fungi, *Aspergillus niveus* and *Alternaria chlamydosporigena*, were tested to assess how well they can clean up Zn and Cd pollution together with biochar in the bioremediation experiment. Third, to understand the adsorption mechanisms of the heavy metals, kinetic and biosorption equilibrium studies were carried out.

## 2. Materials and methods

### 2.1. Sample Collection and Preparation

Soil samples were collected systematically from the upper 20 cm at various contaminated sites in Al-Ahsa and Buqaiq, located in Eastern Saudi Arabia (25°23'N 49°36'E). These sites are known to exhibit heavy metal contamination due to petroleum operations. Pre-sterilized stainless-steel augers were utilized to collect composite samples according to a randomized sampling grid. The samples were homogenized and promptly stored in sterile polythene bags. Samples were kept at 4°C during transport to the laboratory, utilizing insulated iceboxes to ensure microbial longevity, along with avoiding chemical transformation.

### 2.2. Fungal Isolation and Identification

Filamentous fungi were extracted from the soil samples using serial dilution (from  $10^{-1}$  to  $10^{-7}$ ) in sterile phosphate-buffered saline (pH 7.2). For the first step, 1 gram of mixed soil was placed into 10 milliliters of clean distilled water and stirred at 220 rpm for 20 min. The suspension was permitted to sediment for 30 minutes at room temperature (Asomadu *et al.* 2024). Samples of 100  $\mu$ L were spread out in three copies on Potato Dextrose Agar (PDA, HiMedia) with 50 mg/L added.

Fungal colonies were selected according to their morphological characteristics and subsequently subcultured onto fresh PDA plates using quadrant streaking. Pure isolates were stored on PDA slants at 4°C for short-term preservation and in 20% glycerol at -80°C for long-term storage. Chloramphenicol was added to inhibit bacterial growth. Plates were incubated at  $28\pm1$ °C for 5 to 7 days (C. Wang *et al.* 2024). Two isolates were selected based on their superior growth performance in heavy metal-amended potato dextrose broth (200 mg/L Zn or Cd).

Genomic DNA was isolated from fresh mycelia using the CTAB technique, followed by PCR amplification of the internal transcribed spacer (ITS) region employing the universal primers ITS1 (5'-TCCGTAGGTGAACCTGC-3') and ITS4 (5'-TCCTCCGCTTATTGATATGC-3') (Ali *et al.* 2024). The amplified products were sequenced in both directions, and the resulting sequences were submitted to GenBank with accession numbers PQ463633 and PQ463634, respectively. Phylogenetic analysis was

conducted with MEGA X software by matching the ITS sequences with reference strains from NCBI. The maximum likelihood tree, created using 1000 bootstrap repetitions, showed that isolate *PQ463633* is *A. niveus* (99.8% similar to strain CBS 115.57) and isolate *PQ463634* is *A. chlamydosporigena* (99.6% similar to strain CBS 116148) (Figure 1).

### 2.2.1. Metal tolerance of fungi

Following accepted procedures with adaptations, the heavy metal tolerance of *A. niveus* (*PQ4636*) and *A. chlamydosporigena* (*PQ4636*) was assessed by dissolving analytical-grade  $\text{CdCl}_2 \cdot \text{H}_2\text{O}$  (Merck, 99.9%) and  $\text{ZnSO}_4 \cdot 7\text{H}_2\text{O}$  (Sigma-Aldrich, ≥99%) in ultrapure water (Milli-Q, 18.2  $\text{M}\Omega\text{m}$ ), followed by serial dilution in sterile 0.1 M phosphate buffer (pH 6.5) (Amin, Nazir en Rather 2024). Test concentrations ranged from 10–80 ppm. Five-mm mycelial plugs taken from the actively developing margins of the 7-day-old PDA cultures were inoculated onto metal-amended PDA plates ( $n=3$  per concentration) together with metal-free controls for every isolate. For 168 hours, the plates were incubated at  $25 \pm 1^\circ\text{C}$  and  $60 \pm 5\%$  relative humidity. Digital calipers (Mitutoyo, ±0.01 mm precision) and the tolerance index (Ti) were used daily along two perpendicular axes to measure colony diameters;  $\text{Ti} = (\text{R}_1/\text{R}_0) \times 100$  where  $\text{R}_1$  is the mean radial growth in the metal-amended medium and  $\text{R}_0$  is the mean radial growth in the control.

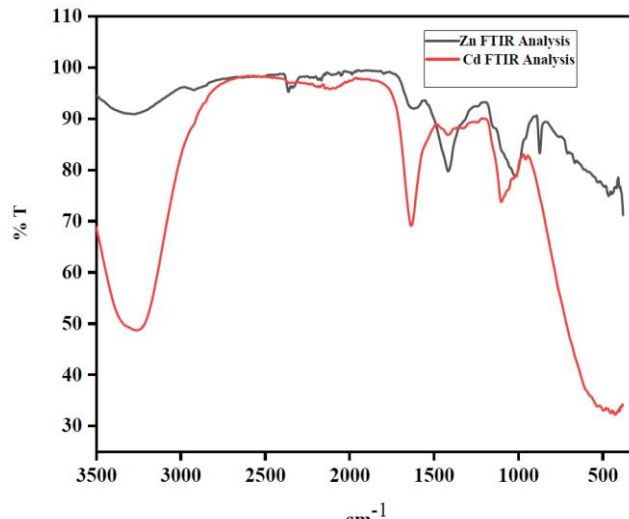


Figure 2. FTIR Study analysis.

### 2.3. Bioremediation experiment

Controlled liquid culture experiments were carried out. To acquire actively proliferating mycelia, fungal isolates were initially cultivated on potato dextrose agar (PDA) plates for 7 days at  $25 \pm 2^\circ\text{C}$ . The experiments were carried out in 250 mL Erlenmeyer flasks that contained 100 mL of potato dextrose broth (PDB) as three replicates. The flasks were supplemented with filter-sterilized aqueous solutions of  $\text{ZnSO}_4 \cdot 7\text{H}_2\text{O}$  and  $\text{CdCl}_2 \cdot \text{H}_2\text{O}$  so that the final metal concentrations were 10, 20, 40, 60, and 80 mg/L. Biochar derived from rice husk (pH 8.2, surface area 230  $\text{m}^2/\text{g}$ ) was obtained from a certified agricultural supplier. Biochar was sterilized through autoclaving and 1.0 g was added to the flasks aseptically. Three 5-mm mycelial discs

from the 7-day-old cultures were aseptically introduced into the flasks. The cultures were maintained at  $25 \pm 1^\circ\text{C}$  with constant agitation (150 rpm) for 7 days. After the incubation, the fungal biomass and biochar were separated via vacuum filtration using a 0.45  $\mu\text{m}$  cellulose membrane, and the filtrate was preserved for residual metal analysis. The fungal biomass was dried in the oven at  $60^\circ\text{C}$  until a constant weight was achieved. The filtrate was acidified with 2%  $\text{HNO}_3$  and analyzed using flame atomic absorption spectrophotometry (AAS; *PerkinElmer PinAAcle 900T*) with detection limits of 0.01 ppm for both metals. Metal removal % was calculated. The treatments were as follows. PDB without amendments (Control), fungal inoculation with either of the two isolates, and fungal isolation with biochar.

### 2.4. Fourier transform infrared spectroscopy (FTIR) analyses

The functional groups of the fungal biomass were analyzed using a Fourier transform infrared spectrometer (*Agilent system Cary 630 FTIR model*). To evaluate the transmittance spectra recorded between  $3000\text{--}400\text{ cm}^{-1}$ , pressed potassium bromide (KBr) pellets were used as depicted in Figure 2.

### 2.5. Kinetic studies and Adsorption isotherm studies.

Lagergren linear pseudo-first-order rate equation found was;

$$\text{Log}(q_e - q_t) = \text{log}q_e - \frac{K_1 t}{2.303} \quad (1)$$

In this context, 'qe' (mg/g) represents the equilibrium adsorption of metal ions, while 'qt' (mg/g) denotes the adsorption at a specific time 't' (min). The rate constant for the pseudo-first-order biosorption process is represented as  $K_1$  ( $\text{min}^{-1}$ ). The results for ' $K_1$ ' and  $q_e$  are presented in Figure 3 displayed on a graph of  $\text{log}(q_e - qt)$  versus time (t) in minutes.

This formulation is utilised to denote the pseudo-second-order model that has been developed.

$$\frac{1}{qt} = \frac{1}{(K_2 q_e 2)} + \frac{1}{q_e} \quad (2)$$

$K_2$  represents the pseudo-second-order equilibrium rate constant measured in g/mg min, while  $q_e$  denotes the quantity of biosorption at equilibrium.

The Langmuir hypothesis posits that sorption takes place at distinct, uniform sites throughout the sorbent material. It is also feasible to articulate non-linear forms of this paradigm.

$$q_e = \frac{q_{mK_1} C_e}{1 + K_1 C_e} \quad (3)$$

In this context, 'qm' denotes the monolayer sorption efficiency of the material (mg/g), while 'Ce' indicates the equilibrium metal ion concentration in the solution (mg/L). The term ' $K_1$ ' refers to the Langmuir adsorption constant (mg/L), which is associated with the free energy of sorption, and 'qe' represents the equilibrium metal ion content of the sorbent (mg/g).

The Freundlich model suggests that the sorption surface exhibits a variety of characteristics. The Freundlich model is

$$q_e = K_f C_e^{1/n} \quad (4)$$

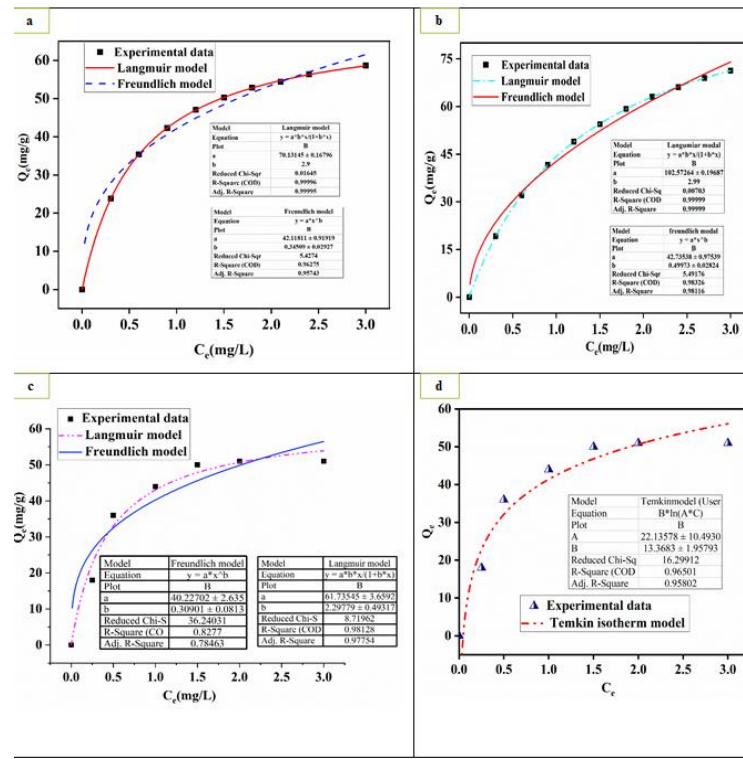


**Figure 3.** Kinetic study analysis. (a) pseudo first order, (b) pseudo second order, (c) Intra particular diffusion, (d)Elovich model.

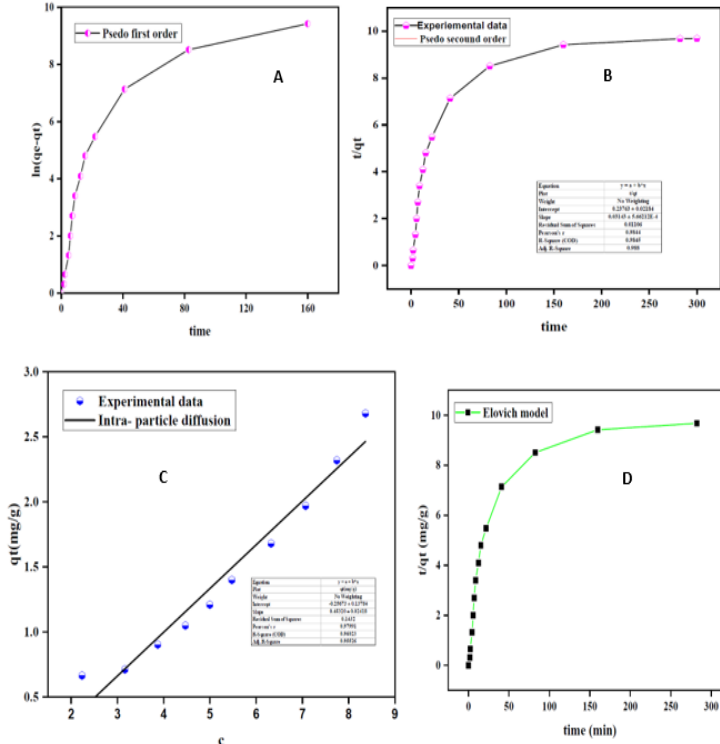


**Figure 4.** Biosorption study analysis. Langmuir: Freundlich: Temkin models.

In this context, 'Kf' represents a constant that characterizes the biosorption capacity, while '1/n' serves as an observational variable. This outlines the degree of biosorption, which varies based on the differences in the material used. The values of 'Kf' and '1/n' were determined

through nonlinear regression analysis. (Figure 4) presents the graphs of the non-linear Freundlich isotherm. The values of '1/n' ranging from '0' to '1' suggest that the biosorption was effective under the examined conditions.

**Table 1.** *A. chlamydosporigena* fungal growth and tolerance index in increasing Zn and Cd concentrations. \* refers to the significant difference to control.

Zn concentration, mg/L	Growth, mm	Tolerance Index
0, Control	7.68±0.07	
10	6.30±0.05	<b>82.10%*</b>
20	5.88±0.16	<b>76.6%*</b>
40	5.45±0.11	<b>70.96%*</b>
60	5.02±0.09	<b>66.23%*</b>
80	4.03±0.08	<b>52.30%*</b>
Cd concentration mg/l.		
0, control	7.68±0.07	
10	6.23±0.03	<b>80.90%*</b>
20	5.49±0.06	<b>71.50%*</b>
40	3.73±0.03	<b>48.00%*</b>
60	3.18±0.24	<b>41.60%*</b>
80	2.18±0.16	<b>28.60%*</b>

**Table 2.** *A. niveus* fungal growth and tolerance index in increasing Zn and Cd concentrations. \* refers to the significant difference from control.

Zn concentration, mg/L	Sample	Zn concentration, mg/L	Tolerance Index
0, Control	6.55±0.05	0, Control	
10	5.72±0.03	10	<b>87.50%*</b>
20	4.50±0.01	20	<b>68.80%*</b>
40	3.20±0.05	40	<b>48.90%*</b>
60	2.72±0.03	60	<b>41.30%*</b>
80	2.55±0.05	80	<b>39.80%*</b>
Cd concentration mg/l.			
0, Control	6.55±0.05	0, Control	--
20	1.77±0.25	20	<b>27.50%*</b>
40	0	40	<b>0*</b>
60	0	60	<b>0*</b>
80	0	80	<b>0*</b>

## 2.6. Statistical Analysis

One-way ANOVAs were carried out using SPSS version 20. Mann Whitney test was used to compare the concentration treatments to the control. The p-value less than 0.05 was assessed as a statistically significant difference.

## 3. Results

### 3.1. Fungal heavy metal tolerance

*Alternaria chlamydosporigena* showed that its growth was affected by the amount of both metals, with Zn causing a noticeable reduction in its growth at all tested levels (10–80 ppm;  $p = 0.050$ ) (**Table 1**). The tolerance indices (Ti) for Zn dropped steadily from 80.9% at 10 ppm to 28.6% at 80 ppm, showing a 64.6% decrease in growth ability. Similarly, exposure to Cd caused a growth reduction, but Ti was higher (82.1% at 10 ppm to 52.3% at 80 ppm), showing that the fungus was more resistant to Cd. One-way ANOVA established the inverse correlation between the metal content and fungal vitality. The rate of growth inhibition was much greater for Zn (slope =  $-0.65\%$  per ppm) compared to Cd (slope =  $-0.37\%$  per ppm).

The growth of *A. niveus* was significantly lower at 10, 20, 40, 60, and 80 ppm than in the control. The tolerance indices for concentrations of 10, 20, 40, 60, and 80 ppm

were 87.50%, 68.80%, 48.90%, 41.30%, and 39.80%, respectively. The growth was significantly reduced at 10, 20, 40, 60, and 80 ppm Cd in comparison to the control. In the Cd concentrations 40 mg/L and higher, no growth was observed. The tolerance indices measured at 10, 20, 40, 60, and 80 ppm were 48.20%, 27.50%, 0%, 0%, and 0%, respectively (**Table 2**).

### 3.2. Heavy metal removal by fungi and biochar

*A. chlamydosporigena* reduced all experimental Zn concentrations significantly. The combined use of *A. chlamydosporigena* and biochar reduced the metals more than the fungus alone. The reduction was 35–55% ( $p = 0.050$ ), being highest at the medium concentrations (40–60 ppm). Significant differences between the treatments ( $F = 8.34$ ,  $p < 0.05$ ) were observed for all concentrations.

The adsorption of zinc and cadmium with *A. niveus* was greatly improved by the addition of biochar at all doses. For zinc, the combination of fungi and biochar consistently showed lower leftover amounts compared to fungi alone, being statistically significant at all tested levels ( $p = 0.050$  at 10/40/60/80 ppm;  $p = 0.046$  at 20 ppm) (**Table 3**). For cadmium, a similar trend was observed, where the combination of fungi and biochar significantly lowered soluble Cd levels ( $p = 0.050$ ) at all concentrations compared to the treatment with only fungi.

**Table 3.** Concentrations of Zinc (Zn) and Cadmium (Cd) in treatments involving *Aspergillus chlamydosporigena* (fungi) and a combination of fungi with biochar under varying Zn concentrations in the culturing medium. \* refers to the significant difference from control.

Zn concentration, mg/L		
Culturing medium	Fungi	Fungi+biochar
0, Control	0.00±0.00	0.00±0.00
10	4.90±0.26	2.03±0.25*
20	9.37±0.57	5.23±0.42*
40	17.20±0.89	10.08±1.07*
60	24.41±0.71	16.40±0.60*
80	38.63±1.18	22.63±0.65*
Cd concentration mg/l.		
Culturing medium	Fungi	Fungi+biochar
0, control	0.00±0.00	0.00±0.00
10	4.40±0.78	2.03±0.25*
20	13.34±0.67	5.23±0.42*
40	24.54±0.67	10.08±1.07*
60	37.87±1.13	16.40±0.60*
80	53.55±0.45	22.63±0.65*

**Table 4.** Zinc (Zn) and Cadmium (Cd) concentrations in treatments with *A. niveus* (fungi) and fungi combined with biochar under increasing Zn concentrations in the culturing medium. \* refers to the significant difference from control.

Zn concentration, mg/L		
Zn concentration mg/l	Fungi+Zn	Fungi+Zn+biochar
0, Control	0.00±0.00	0.00±0.00
10	1.85±0.44	0.18±0.07*
20	3.93±0.96	0.42±0.03*
40	8.53±0.61	5.10±0.6*
60	24.08±1.03	8.77±0.25*
80	23.37±3.73	12.07±0.21*
Cd concentration mg/l		
Cd concentration mg/l	Fungi+Cd	Fungi+Cd+biochar
0, Control	0.00±0.00	0.00±0.00
10	1.85±0.44	0.18±0.07*
20	3.93±0.96	0.42±0.03*
40	8.53±0.61	5.10±0.6*
60	24.08±1.03	8.77±0.25*
80	23.37±3.73	12.07±0.21*

### 3.3. FTIR Analysis

The biggest changes were seen in the range of 1800-1200  $\text{cm}^{-1}$ , where carboxylate groups ( $\text{COO}^-$ ) shifted down in frequency by 1822  $\text{cm}^{-1}$  during their symmetric stretching vibrations (from 1420 to 1398  $\text{cm}^{-1}$  for Zn and from 1420 to 1402  $\text{cm}^{-1}$  for Cd) in (Figure 2). The decrease (34%) in the peak intensity of carbonyl ( $\text{C=O}$ ) at 1720  $\text{cm}^{-1}$  was observed. Protein components showed 12-15% widening in the amide I (1650  $\text{cm}^{-1}$ ) and amide II (1540  $\text{cm}^{-1}$ ) bands. Shoulders appeared around 1580-1560  $\text{cm}^{-1}$ , which is indicative of metal-nitrogen bonding. Stronger phosphoryl ( $\text{P=O}$ ) signals at 1220  $\text{cm}^{-1}$  and stronger vibrations from polysaccharides at 1050  $\text{cm}^{-1}$  were observed. Zn-O vibration at 620  $\text{cm}^{-1}$  and Cd-S at 550  $\text{cm}^{-1}$  were observed in Zn and Cd treatments, respectively.

### 3.4. Kinetic Studies

The pseudo-first-order model assumes that each metal ion attaches to one specific spot on the surface of the biosorbent. The pseudo-second-order correlation coefficient ( $R^2$ ) values are relatively high (Figure 3). The biosorption process, which follows chemisorption as a

second-order reaction, is represented by the linear formulation provided above.

### 3.5. Biosorption Isotherm Models

The Langmuir model demonstrated the greatest fit to the experimental data ( $R^2 > 0.98$ ), followed by the Freundlich model ( $R^2 = 0.92-0.95$ ) and the Temkin model ( $R^2 = 0.85-0.89$ ). The Langmuir analysis showed the maximum adsorption capacities ( $q_{\text{max}}$ ) for Zn (II) and for Cd (II). Furthermore, the affinity constants ( $K_1$ ) were high. Dimensionless separation factors ( $R_1$ ) ranged from 0.02 to 0.35. The Freundlich model exhibited a somewhat weaker correlation, with its heterogeneity value ( $1/n = 0.42-0.58 < 1$ ). According to the Temkin model, moderate adsorption heats were observed ( $b_2 = 120-180 \text{ J/mol}$ ).

### 3.6. Discussion

The two native fungal isolates were efficient in reducing Zn and Cd concentrations. However, the leftover metal concentrations were still too high when either of the fungi was incubated. This showed that the natural ability of the fungi to remove metals was limited. It is known that certain species can adsorb heavy metals. These fungi have

often been isolated from heavy metal-polluted sites such as *A. terreus* and *A. hiratsukae* in Oman (Palanivel, Pracejus en Novo 2023). Moreover, other pollution seems to induce the stress-resistance of fungi. Several *Aspergillus* species have shown to adsorb Cr, Zn, Cu, Cd, and Ni efficiently (Vašinková, Dlabaja en Kučová 2021; Narolkar, Jain en Mishra 2022). The heavy metal-resistant strain of *A. flavus* was isolated from an oil-polluted soil (Al-Dhabaan 2022). It has also been found that the combined pollution of heavy metals and oil generates resistant fungal strains. The efficiency of these fungi to adsorb pollutants is due to the secreted extracellular enzymes and other metabolites (Li, Liu en Gadd 2020).

The efficiency of metal reduction was increased remarkably when rice husk biochar was added together with the fungi. The system exhibited its highest efficiency at the concentration of 40 ppm, removing 86.5% Zn and 89.2% Cd. We interpret that *A. chlamydosporigena* alone is not enough efficient to reduce the metal concentrations, but together with biochar, the remediation process is highly efficient. This is due to the three benefits that biochar provides: (i) supplementary binding sites, (ii) toxicity buffering for fungal cells, and (iii) pH stabilization with the final pH of 6.8 (Chen *et al.* 2022).

Based on the consistent patterns observed, it can be inferred that biochar contributes through various mechanisms (Gorovtsov *et al.* 2020). Firstly, it offers additional adsorption sites through its porous matrix. Secondly, it alters the metal speciation by elevating the pH level. Lastly, biochar has the potential to protect fungal biomass from the harmful effects of metals. In our study, the ability of biochar to improve fungal cleanup was shown to be effective at all concentrations, with the most effective at 20 ppm Zn. Specifically, in moderately Zn-contaminated systems (20–60 ppm), biochar increased metal immobilization by 38–52% compared to fungal treatment alone. Our findings established that rice husk biochar was an efficient amendment for *A. niveus*-based bioremediation.

FTIR provided molecular-level evidence of the mechanisms that underlie heavy metal biosorption in the fungal-biochar systems (Racić *et al.* 2023; Nandasana, Thongmee en Ghosh 2024). After comparing the spectral profiles of biomass exposed to metals and those that were not, it was found that important functional groups changed. Carboxylate (COO<sup>-</sup>) and carbonyl (C=O) groups shifted down in frequency. These alterations provide further evidence that carboxyl groups play an essential part in the coordination of metals through intramolecular interactions. Protein components showed important changes in structure, shown by a 12–15% widening of the bands of amides. Moreover, metal-nitrogen bonding was observed. Spectral fingerprints that were unique to the fungal-biochar composites were observed previously (Zhao *et al.* 2024). These unique signals included stronger phosphoryl and polysaccharides signals indicating the creation of ternary complexes between the fungal cell walls, metals, and biochar surfaces. The metal-specific signatures were particularly noteworthy. The exposure to

zinc resulted in the generation of a distinct Zn-O vibration at 620 cm<sup>-1</sup>. The treatment with cadmium resulted in the production of a Cd-S stretching band at 550 cm<sup>-1</sup>. This suggests that Zn has a preference for oxygen-dominated coordination, whereas Cd was involved in sulfur participation (Nandasana, Thongmee, and Ghosh 2024). The spectroscopic evidence as a whole demonstrates that biochar improves the process of metal sequestration in fungi by the following mechanisms: (i) protecting essential fungal binding sites from the toxicity of metals; (ii) introducing additional oxygen-containing functional groups; and (iii) facilitating the formation of stable ternary complexes. These molecular-scale interactions provide an explanation for the reported 35–55% boost in metal removal efficiency that occurs when biochar amendment is combined with fungal therapy.

Kinetic studies are crucial for clarifying the reaction mechanisms and rates of solute absorption in biosorption processes. This is especially true in bioremediation systems that are aimed to reduce heavy metals such as Zn and Cd (Karnwal 2024; Mir en Rather 2024). The findings from these studies provide important information about how metal ions interact with biosorbents like biochar or fungal biomass at the surface where solid and liquid meet. These dynamics have a direct impact on the effectiveness of contaminant removal. In the framework of this investigation, pseudo-first-order and pseudo-second-order models were utilized to assess the biosorption kinetics of Zn and Cd by biochar and fungi (Xie 2024). The pseudo-first-order model assumes that each metal ion attaches to one specific spot on the surface of the biosorbent (Al-Homaidan *et al.* 2018). On the other hand, the pseudo-second-order model proposes the existence of chemisorption mechanisms, in which adsorption is characterized by the presence of shared active sites or contacts that are influenced by electrostatic forces, chemical bonding, or ion exchanges. The pseudo-second-order model is typically more suitable for estimating bioremediation kinetics. This advantage is due to the fact that heavy metal biosorption frequently follows chemisorption, which is a process of the second order (P. Wang *et al.* 2024).

Comprehending the kinetics of metal biosorption is crucial for enhancing bioremediation strategies in oil-contaminated environments, as it offers vital information regarding the efficiency, mechanism, and scalability of the process. Kinetic parameters, including  $K_1$ ,  $K_2$ , and  $q_e$ , are essential for quantifying the rate and extent of metal removal. This quantification facilitates the design of efficient large-scale remediation systems. A high correlation coefficient ( $R^2$ ) for the pseudo-second-order model, aligning with findings from analogous studies on Cu, suggests that chemisorption is the primary mechanism for the uptake of Zn and Cd by biochar and fungi. The involvement of functional groups, such as carboxyl and hydroxyl, found in fungal cell walls and biochar surfaces supports this process by facilitating metal binding through chemical interactions. Kinetic data also establish the necessary residence time for both batch and continuous-

flow systems, facilitating effective and efficient implementation in oilfield remediation.

Isotherm models help us understand how the biosorbents attract and hold onto metals, their surface features, and how much metal they can absorb at most (Mir en Rather 2024; Sarangi en Rajkumar 2024). The results showed that monolayer adsorption was the predominant mode of action in the biosorption process. The Langmuir analysis showed the maximum adsorption capacities. Furthermore, the affinity constants were high, which indicated that there were significant interactions between the metal and the biosorbent. Further confirmation of the favorable adsorption conditions was provided by dimensionless separation factors. Despite the fact that the Freundlich model exhibited a somewhat weaker correlation, its heterogeneity value indicated a certain degree of multilayer adsorption and surface heterogeneity. This is most likely due to the porous structure of biochar and the different functional groups that are present on fungal biomass (Medina-Armijo *et al.* 2024). According to the Temkin model, moderate adsorption heats were observed, which suggests that electrostatic interactions play a role in the binding mechanism.

These data collectively show that chemisorption is the major adsorption mechanism and that it occurs through mechanisms such as ion exchange and surface complexation. However, it is important to note that there is some variation in the binding site energies because of these discoveries. This validates the creation of a homogeneous monolayer of metal ions on the biosorbent surfaces, which is essential for forecasting and optimizing remediation effectiveness in field applications. The superior fit of the Langmuir model has important practical consequences since it confirms the formation of this monolayer. This biochar-fungal system has a strong potential for effective heavy metal removal from contaminated oil sites, as demonstrated by the high  $q_{\text{mas}}$  values that were obtained. Additionally, the secondary Freundlich characteristics indicate that there are opportunities for further enhancement through modification of surface properties in order to take advantage of multilayer adsorption. These findings highlight the significance of isotherm analysis for gaining knowledge and improving contaminant removal processes, offering substantial insights that can be utilized in developing effective bioremediation strategies (Meena *et al.* 2018). A homogenous, monolayer-driven biosorption of the metals is highlighted by the best-fit state of the Langmuir isotherm. On the other hand, the Freundlich and Temkin models offer supplementary insights into surface heterogeneity and interaction energies.

It has been shown that fungi and biochar have synergistic effects in the remediation of different pollutants. The combination was efficient to remediate the combined pollution of organic pollutants and heavy metals (Xia *et al.* 2025). Elsewhere, biochar and bacteria were shown to be efficient in the remediation of oil-contaminated soil (Li *et*

*al.* 2025). Moreover, biochar and fungi were efficient in remediating various pollutants (Pai *et al.* 2024). Our results support the previous findings that biochar-fungal systems are effective for the removal of heavy metals, and thus, we can provide recommendations for the development of future strategies.

When used with fungal biomass, biochar's large surface area ( $230 \text{ m}^2/\text{g}$ ) and ability to exchange cations ( $24.5 \text{ cmol}^+/\text{kg}$ ) led to more metal being absorbed. This was accomplished through both physical binding and chemical interactions (Awasthi *et al.* 2021). In subsequent research, it is recommended to explore the long-term metal stability and field-scale performance of this consortium consisting of biochar and plants.

### 3.7. Conclusion and Recommendations

The findings of this study show that the local fungi *A. niveus* (PQ463633) and *A. chlamydosporigena* (PQ463634) could effectively clean up soils contaminated with zinc and cadmium in eastern Saudi Arabia. Adsorption isotherm analysis confirmed Langmuir monolayer adsorption as the major mechanism, with the Freundlich and Temkin models indicating additional heterogeneous binding interactions. The isolates displayed remarkable metal resistance and biosorption capacity. Kinetic studies showed that the metals were taken up quickly, and Fourier transform infrared spectroscopy revealed that the metals were actively bound through interactions with functional groups. A promising combined approach for real-world use is shown by the improved cleanup effectiveness gained by adding biochar. The selected fungal strains were able to remove significant amounts of heavy metals by simultaneously utilizing a combination of biosorption and bioaccumulation mechanisms, and the addition of biochar resulted in a considerable improvement in the efficacy of the remediation process by increasing the immobilization of metals. The balance of the data was best explained by the Langmuir isotherm model, showing that chemisorption was the main process at work.

Furthermore, the genetic and proteomic investigations may elucidate the molecular resistance mechanisms of these fungal species. The study's results establish a foundation for environmentally friendly, nature-based remediation technologies that may supplant energy-intensive methods in oil-contaminated regions. Subsequent research should investigate the scalability of this strategy and evaluate the regulatory frameworks necessary for its implementation.

### Author Contributions

The final draft of the work has been reviewed and approved by all authors.

### Conflict of interest

The authors declare that they have no conflicts of interest.

### Acknowledgments

The authors extend their appreciation to the ongoing research funding program (ORF-2025-364), King Saud University, Riyadh, Saudi Arabia.

## References

- Al-Dhabaan, F.A. (2022) "Characterization of Cadmium and Lead Heavy Metals Resistant Fungal Isolates from Ghawar oil field, Saudi Arabia", *Biosciences Biotechnology Research Asia*, 19(3), bll 625–633. Available at: <https://doi.org/10.13005/bbra/3015>.
- Al-Homaidan, A.A. et al. (2018) "Potential use of green algae as a biosorbent for hexavalent chromium removal from aqueous solutions", *Saudi Journal of Biological Sciences*, 25(8), bll 1733–1738. Available at: <https://doi.org/10.1016/j.sjbs.2018.07.011>.
- Ali, S.A. et al. (2024) "the Endophytic Fungus Epicoccum Nigrum: Isolation, Molecular Identification and Study Its Antifungal Activity Against Phytopathogenic Fungus Fusarium Solani", *Journal of Microbiology, Biotechnology and Food Sciences*, 13(5), bll 10093– 10093. Available at: <https://doi.org/10.55251/jmbfs.10093>.
- Almutairi, H. (2024). Microbial communities in petroleum refinery effluents and their complex functions. *Saudi Journal of Biological Sciences*. <https://doi.org/10.1016/j.sjbs.2024.104008>.
- Ameen, F., Alsarraf, M., Abalkhail, T. Stephenson, S. (2024). Evaluation of resistance patterns and bioremoval efficiency of hydrocarbons and heavy metals by the mycobiome of petroleum refining wastewater in Jazan with assessment of molecular typing and cytotoxicity of *Scedosporium apiospermum* JAZ-20. *Heliyon*. <https://doi.org/10.1016/j.heliyon.2024.e32954>.
- Amin, I., Nazir, R. en Rather, M.A. (2024) "Evaluation of multi-heavy metal tolerance traits of soil-borne fungi for simultaneous removal of hazardous metals", *World Journal of Microbiology and Biotechnology*, 40(6), bl 175. Available at: <https://doi.org/10.1007/s11274-024-03987-z>.
- Asomadu, R.O. et al. (2024) "Exploring the antioxidant potential of endophytic fungi: a review on methods for extraction and quantification of total antioxidant capacity (TAC)", *3 Biotech*, bl 127. Available at: <https://doi.org/10.1007/s13205-024-03970-3>.
- Awasthi, S.K. et al. (2021) "Sequential presence of heavy metal resistant fungal communities influenced by biochar amendment in the poultry manure composting process", *Journal of Cleaner Production*, 291, bl 125947. Available at: <https://doi.org/10.1016/j.jclepro.2021.125947>.
- Chen, L. et al. (2022) "Removal of heavy-metal pollutants by white rot fungi: Mechanisms, achievements, and perspectives", *Journal of Cleaner Production*, 354, bl 131681. Available at: <https://doi.org/10.1016/j.jclepro.2022.131681>.
- Dhaka, R. et al. (2024) "Biosorption of lead (II) ions by lead-tolerant fungal biomass isolated from electroplating industry effluent", *International Journal of Environmental Science and Technology*, 22(5), bll 2955–2966. Available at: <https://doi.org/10.1007/s13762-024-05796-1>.
- Dinakarkumar, Y. et al. (2024) "Fungal bioremediation: An overview of the mechanisms, applications and future perspectives", *Environmental Chemistry and Ecotoxicology*, 6, bll 293–302. Available at: <https://doi.org/10.1016/j.enceco.2024.07.002>.
- Falih, K.T. et al. (2024) "Assessment of petroleum contamination in soil, water, and atmosphere: a comprehensive review", *International Journal of Environmental Science and Technology*, 21(13), bll 8803–8832. Available at: <https://doi.org/10.1007/s13762-024-05622-8>.
- Gorovtsov, A. V. et al. (2020) "The mechanisms of biochar interactions with microorganisms in soil", *Environmental Geochemistry and Health*, 42(8), bll 2495–2518. Available at: <https://doi.org/10.1007/s10653-019-00412-5>.
- Hou, D. et al. (2025) "Global soil pollution by toxic metals threatens agriculture and human health", *Science (New York, N.Y.)*, 388(6744), bll 316–321. Available at: <https://doi.org/10.1126/science.adr5214>.
- Karnwal, A. (2024) "Unveiling the promise of biosorption for heavy metal removal from water sources", *Desalination and Water Treatment*, 319, bl 100523. Available at: <https://doi.org/10.1016/j.dwt.2024.100523>.
- Li, Q., Liu, J. en Gadd, G.M. (2020) "Fungal bioremediation of soil co-contaminated with petroleum hydrocarbons and toxic metals", *Applied Microbiology and Biotechnology*, 104(21), bll 8999–9008. Available at: <https://doi.org/10.1007/s00253-020-10854-y>.
- Li, X. et al. (2025) "Synergistic biochar-microbe interactions enhance petroleum contaminant removal and microbial community succession", *Environmental Technology and Innovation*, 40, bl 104465. Available at: <https://doi.org/10.1016/j.eti.2025.104465>.
- Liu, X. et al. (2024) "Frontiers in Environmental Cleanup: Recent Advances in Remediation of Emerging Pollutants from Soil and Water", *Journal of Hazardous Materials Advances*, bl 100461. Available at: <https://linkinghub.elsevier.com/retrieve/pii/S2772416624000627>.
- Medina-Armijo, C. et al. (2024) "The Metallotolerance and Biosorption of As(V) and Cr(VI) by Black Fungi", *Journal of Fungi*, 10(1), bl 47. Available at: <https://doi.org/10.3390/jof10010047>.
- Meena, R.A.A. et al. (2018) "Heavy metal pollution in immobile and mobile components of lentic ecosystems—a review", *Environmental Science and Pollution Research*, 25(5), bll 4134–4148. Available at: <https://doi.org/10.1007/s11356-017-0966-2>.
- Mir, D.H. en Rather, M.A. (2024) "Kinetic and thermodynamic investigations of copper (II) biosorption by green algae Chara vulgaris obtained from the waters of Dal Lake in Srinagar (India)", *Journal of Water Process Engineering*, 58, bl 104850. Available at: <https://doi.org/10.1016/j.jwpe.2024.104850>.
- Nandasana, M., Thongmee, S. en Ghosh, S. (2024) "Microbial Biochar Based Sustainable Waste Management Approach", in *Environmental Science and Engineering*. Cham: Springer International Publishing, bl 121–145. Available at: [https://doi.org/10.1007/978-3-031-62898-6\\_6](https://doi.org/10.1007/978-3-031-62898-6_6).
- Narolkar, S., Jain, N. en Mishra, A. (2022) "Biosorption of Chromium by Fungal Strains Isolated from Industrial Effluent Contaminated Area", *Pollution*, 8(1), bll 159–168. Available at: <https://doi.org/10.22059/POLL.2021.326818.1132>.
- Nna, P.J., Orie, K.J. en Kalu, N.A.S. (2024) "Source Apportionment and Health Risk of Some Organic Contaminants in Water and Suspended Particulate Matter from Imo River, Nigeria", *Journal of Applied Sciences and Environmental Management*, 28(2), bll 291–303. Available at: <https://doi.org/10.4314/jasem.v28i2.1>.
- Pai, S. et al. (2024) "Synergistic interactions of fungi and biochar for various environmental applications", in *Bioprospecting of Multi-tasking Fungi for a Sustainable Environment: Volume I*.

- Singapore: Springer Nature Singapore, bl 219–247. Available at: [https://doi.org/10.1007/978-981-97-4113-7\\_10](https://doi.org/10.1007/978-981-97-4113-7_10).
- Palanivel, T.M., Pracejus, B. en Novo, L.A.B. (2023) "Bioremediation of copper using indigenous fungi *Aspergillus* species isolated from an abandoned copper mine soil", *Chemosphere*, 314, bl 137688. Available at: <https://doi.org/10.1016/j.chemosphere.2022.137688>.
- Racić, G. et al. (2023) "Screening of Native *Trichoderma* Species for Nickel and Copper Bioremediation Potential Determined by FTIR and XRF", *Microorganisms*, 11(3), bl 815. Available at: <https://doi.org/10.3390/microorganisms11030815>.
- Sarangi, N.V. en Rajkumar, R. (2024) "Biosorption potential of *Stoechospermum marginatum* for removal of heavy metals from aqueous solution: Equilibrium, kinetic and thermodynamic study", *Chemical Engineering Research and Design*, 203, bl 207–218. Available at: <https://doi.org/10.1016/j.cherd.2024.01.020>.
- Vašinková, M., Dlabaja, M. en Kučová, K. (2021) "Bioaccumulation of toxic metals by fungi of the genus *Aspergillus* isolated from the contaminated area of Ostramo Lagoons", *IOP Conference Series: Earth and Environmental Science*, 900(1), bl 12048. Available at: <https://doi.org/10.1088/1755-1315/900/1/012048>.
- Wang, C. et al. (2024) "Isolation and Identification of Pear Ring Rot Fungus and Resistance Evaluation of Different Pear Varieties", *Horticulturae*, 10(11). Available at: <https://doi.org/10.3390/horticulturae10111152>.
- Wang, P. et al. (2024) "Bio-sorption capacity of cadmium and zinc by *Pseudomonas monteili* with heavy-metal resistance isolated from the compost of pig manure", *Bioresource Technology*, 399, bl 130589. Available at: <https://doi.org/10.1016/j.biortech.2024.130589>.
- Wang, W. et al. (2024) "Biochar remediates cadmium and lead contaminated soil by stimulating beneficial fungus *Aspergillus* spp.", *Environmental Pollution*, 359, bl 124601. Available at: <https://doi.org/10.1016/j.envpol.2024.124601>.
- Xia, Y. et al. (2025) "An efficient fungi-biochar-based system for advancing sustainable management of combined pollution", *Environmental Pollution*, 367, bl 125649. Available at: <https://doi.org/10.1016/j.envpol.2025.125649>.
- Xie, S. (2024) "Biosorption of heavy metal ions from contaminated wastewater: an eco-friendly approach", *Green Chemistry Letters and Reviews*, 17(1), bl 2357213. Available at: <https://doi.org/10.1080/17518253.2024.2357213>.
- Zhao, Z. et al. (2024) "Combined microbe-plant remediation of cadmium in saline-alkali soil assisted by fungal mycelium-derived biochar", *Environmental Research*, 240, bl 117424. Available at: <https://doi.org/10.1016/j.envres.2023.117424>.